CrystEngComm

Accepted Manuscript

This is an *Accepted Manuscript*, which has been through the Royal Society of Chemistry peer review process and has been accepted for publication.

Accepted Manuscripts are published online shortly after acceptance, before technical editing, formatting and proof reading. Using this free service, authors can make their results available to the community, in citable form, before we publish the edited article. We will replace this *Accepted Manuscript* with the edited and formatted *Advance Article* as soon as it is available.

You can find more information about *Accepted Manuscripts* in the Information for Authors.

Please note that technical editing may introduce minor changes to the text and/or graphics, which may alter content. The journal's standard Terms & Conditions and the Ethical guidelines still apply. In no event shall the Royal Society of Chemistry be held responsible for any errors or omissions in this *Accepted Manuscript* or any consequences arising from the use of any information it contains.

ROYAL SOCIETY OF CHEMISTRY

www.rsc.org/crystengcomm

Journal Name

RSCPublishing

COMMUNICATION

Growth mechanism of apatite nanocrystals assisted by citrate: relevance to bone biomineralization

Cite this: DOI: 10.1039/x0xx00000x

Received 00th January 2012,
Accepted 00th January 2012

DOI: 10.1039/x0xx00000x

www.rsc.org/

Michele Iafisco,*[,a] Gloria Belén Ramírez-Rodríguez,[a,b] Yuriy Sakhno,[c] Anna Tampieri,[a] Gianmario Martra,[c] Jaime Gómez-Morales,[b] and José Manuel Delgado-López*[,b]

Here we report that citrate plays a key dual role in the apatite crystallization: driving a growth pathway via an amorphous precursor and controlling the size of nanocrystals by the non-classical oriented aggregation mechanism. These results provide new insights in bone mineralization, where the role of citrate might be wider than has been thought to date.

In Nature, composite materials show complex hierarchical organization with highly organized nanometric building blocks that improve their functionalities.[1] The classical model of crystal growth in biomineralization considers mineral formation as a process in which atoms or molecules add to existing nuclei or templates and proteins and peptides can control nucleation, growth, and facet stability.[2] This concept has been challenged in the last years by the non-classical crystallization theory of aggregation-based crystal growth.[3] Banfield and Penn demonstrated in 90's that inorganic nanocrystals could aggregate into ordered solid phases via oriented aggregation (OA) or grain growth and coalescence to control the reactivity of the nano-phases.[3] The arrangement can be obtained with the fusion of primary blocks since they share a common crystallographic orientation.[3]

Apatite (Ap) is the mineral phase of mammals bone and teeth.[1b] Despite its importance and the effort of scientific community, Ap crystallization in biological tissues is still far to be fully comprehended. Synthetic Ap can form long nanocrystals through OA when prepared by hydrothermal synthesis[4] and well-organized assemblies of Ap nanocrystals when synthesised in biomimetic conditions in presence of organic molecules.[5] In these latter cases, the formation of long enamel-like crystals with their nano-sized subunits attached along the *c*-axis involves the formation of amorphous calcium phosphate (ACP, $Ca_3(PO_4)_2$) as precursor.[5a] ACP phase can serve as mortar in a "bricks and mortar" model to cement the subunits once they have oriented into crystallographic register by control of biomolecules.[5a] Such biomolecules are aminoacids like glycine, arginine and aspartic acid or proteins like amelogenin.[5]

Nowadays the connection between Ap and citrate is complex and is the subject of much interest.[6] It was proposed that citrate populating the surface of bone Ap nanocrystals limits their further growth and renders the mineral surface more hydrophobic to interact with collagen.[6a,7] It is unclear if the abundance of citrate in bone may reflect its necessary participation in the mineralization process, or its presence may be coincidental and reflects the high affinity of the citrate for calcium at physiological pH. Therefore, the aim of this paper is to elucidate the effect of citrate as control molecule for the Ap crystallization to highlight its possible role in biomineralization.

Ap nanoparticles were precipitated in presence of citrate by a batch heating method according to the procedure reported by Delgado-Lopez et al.[6c] (See ESI† for details). The crystallization experiments were stopped at different maturation times ranging from 30 s to 96 h and the resulting materials were dried and analysed by X-ray powder diffraction (XRPD), transmission electron microscopy (TEM), including high resolution (HR-TEM), and atomic force microscopy (AFM). Experiments without citrate were also carried out for the sake of comparison.

XRPD patterns of the samples precipitated at different times (Fig. S1, ESI†) show that the crystallization pathway started with the formation of ACP that progressively transformed to Ap containing adsorbed citrate (cit-Ap). These samples exhibited higher crystallinity degree and ordered structure at increasing maturation time. In the absence of citrate the hydroxyapatite formation occurred through a different route (Fig. S2, ESI†). After 30 s the presence of dicalcium phosphate dihydrate or brushite (DCPD, $CaHPO_4{\cdot}2H_2O$) and poorly crystalline Ap was pointed out by XRPD analysis. As a function of time the diffraction peaks of DCPD completely disappeared, while in turn peaks of octacalcium phosphate (OCP, $Ca_8H_2(PO_4)_6{\cdot}5H_2O$) emerged. Finally, this phase transformed into hydroxyapatite (as suggested by the decrease in intensity of the characteristic double reflections at 9.44 and 9.77° 2θ typical of the (02-20) and (11-20) planes of OCP).[8]

Fig. 1 shows TEM micrographs and selected area diffraction (SAED) patterns of the cit-Ap samples precipitated at increasing maturation times. At early precipitation time (30 s), aggregated particles of 50-100 nm in diameter were observed and the SAED pattern confirmed their amorphous nature (Fig. 1a). Previous AFM

CrystEngComm Accepted Manuscript

observations revealed that they are rounded platelets exhibiting fairly unusual thickness much smaller than both their average length and width.[9] At increasing maturation times, elongated particles with progressively better-defined border and with increased crystallinity, as evidenced by SAED patterns, appeared (Figs. 1b-d). On the contrary, TEM images of the precipitates after 30 s using the citrate-free solutions showed well-defined plate-like DCPD crystals (Fig. S3a, ESI†) and Ap nanoparticles (Fig. S3b, ESI†). After 5 min, elongated platelets of OCP crystals originated from the hydrolysis of DCPD were clearly observed (Fig. S3c, ESI†). Increasing the maturation time up to 96 h the major part of the sample was composed of long hydroxyapatite crystals most probably coming from the OCP hydrolysis (Fig. S3d, ESI†).

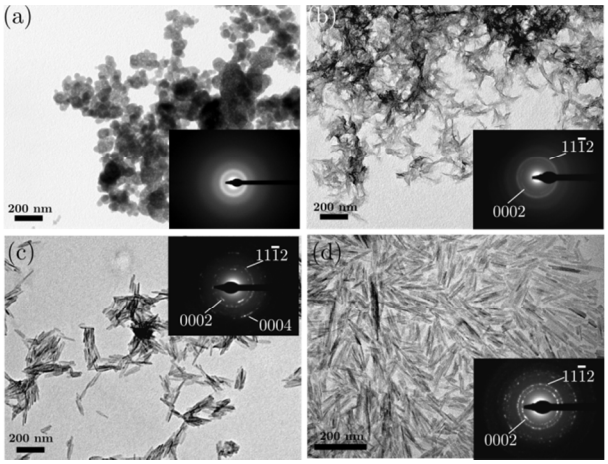

Fig. 1. TEM micrographs of cit-Ap after 30 s (a), 5 min (b), 4 hours (c) and 96 hours (d) of maturation. Insets: corresponding SAED patterns. Original magnification: 75k×

The pH variation during the reactions was monitored (Fig. S4, ESI†) evidencing that both experiments were accompanied by the initial fast drop in pH due to the formation of acidic species. After that the pH remained stable. During the cit-Ap crystallization the drop of pH was lower and faster (from 8.5 to 6.7 in 5 min) than in the experiments without citrate (from 8.5 to 4.9 in 25 min). In presence of citrate in the first 5 min two events took place: the instantaneous formation of ACP, that can be stabilized by citrate adsorption,[10] and its subsequent transformation to Ap causing the release of H^+ (simplified reaction 1)

$$3Ca_3(PO_4)_2+Ca^{2+}+2H_2O\rightarrow 2Ca_5(PO_4)_3(OH)+2H^+ \quad (1)$$

Conversely, in the absence of citrate the initial formation of DCPD and its transformation to OCP was followed by the conversion of OCP to hydroxyapatite (simplified reactions 2 and 3). These reactions generate $H2PO_4^-$ and HPO_4^{2-} species:

$$10CaHPO_4\cdot 2H_2O\rightarrow Ca_8H_2(PO_4)_6\cdot 5H_2O+2Ca^{2+}+4H_2PO_4^-+15H_2O \quad (2)$$

$$Ca_8H_2(PO_4)_6\cdot 5H_2O\rightarrow Ca_5(PO_4)_3(OH)+3Ca^{2+}+3HPO_4^{2-}+4H_2O \quad (3)$$

It is worth mentioning that the two crystallization pathways were not driven by the different pH evolutions but most probably they were caused by the ability of citrate to stabilize the ACP phase. In fact, although after 30 s the pH values were the same, different phases were detected (ACP and DCPD/Ap in the presence and in the absence of citrate, respectively (Figs. 1A and S3A, ESI†).

Supersaturation index of the calcium phosphate (CaP) phases in presence and in absence of citrate (Table S1, ESI†) indicated that citrate caused a decrease of free calcium ions in solution with the resulting reduction of the supersaturation of all the CaP phases. However, in both cases the systems were supersaturated with respect to hydroxyapatite rather than the other CaP phases (including ACP). Therefore the reduction of calcium concentration by citrate complexation was unlikely to be the responsible for the ACP formation, as also previously reported.[10]

The ACP-mediated crystallization of Ap in presence of citrate was in agreement with the work of Delgado-Lopez et al.[9] In this work, size and shape of the crystal domains were analysed by synchrotron X-Ray total scattering (XRTS) and compared to those of multi-domain Ap nanoparticles observed by AFM. They found that the initial precipitation of sodium citrate crystals acted as temporal templates, triggering heterogeneous nucleation of ACP with unusual platy shape. Then, ACP nanoparticles, stabilized by the adsorption of citrate ions, were progressively transformed into platy Ap nanoparticles.[9] Therefore citrate played the distinct role of inducing the platy morphology of the amorphous precursor and controlling the thickness of the Ap nanocrystals, breaking their hexagonal symmetry.[9]

It was proposed that the Ap crystallization pathway involving an ACP precursor could be one of the most important mechanism in biomineralization.[1,11] However, the role of organic molecules and the growth pathway is still not completely clear. A comprehensive morphological characterization is necessary to elucidate these processes and it is recognized that one of the most suitable methods is the observation of the crystals by HR-TEM.[12]

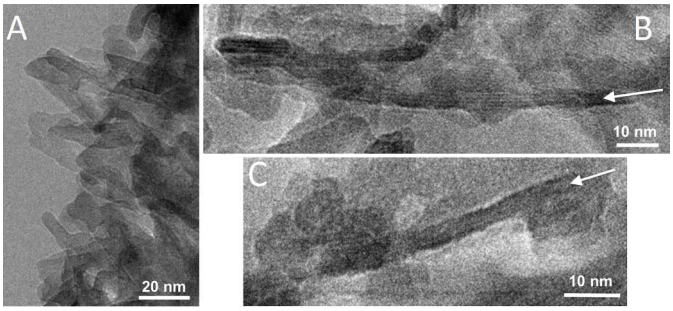

Fig. 2. HR-TEM images representative of the overall aspect of cit-Ap-1h. Original magnification: 150k×.

Representative HR-TEM images of cit-Ap obtained after 1 h of maturation (cit-Ap-1h) are reported in Fig. 2. This material appeared in most of the cases constituted of particles producing on the image plane platy projections of about 10-20 nm in length and 5-10 nm width. Only in few cases lattice fringes spaced of ca. 0.815 nm turned up. This lattice fringe value corresponds to the distance of (10-10) plane of hydroxyapatite (JCPDS file no. 9-432) indicating that the crystals are elongated towards the *c*-axis. Noticeably, in some cases, they seemed aligned along the *c*-axis forming uniaxially aggregated crystals of about 40-50 nm (white arrows in Figs. 2B,C).

HR-TEM images of cit-Ap maturated after 4 h (cit-Ap-4h) (Fig. 3) confirmed the formation of oriented aggregates. Indeed, most of the

CrystEngComm Accepted Manuscript

This journal is © The Royal Society of Chemistry 2012

particles were composed of smaller head-tail connected subunits whose primary size lied in the range of 5-15 nm (Fig. 3A,B). The lengths of primary units were in agreement with those of the crystal domains determined by XRTS (16.7 ± 7.9, data extract from reference 9). In this sample the 0.815 nm fringes were more clearly and frequently observed than in the cit-Ap-1h confirming the increased crystallinity and the ordered structure of these nanoparticles (Fig. 3C).

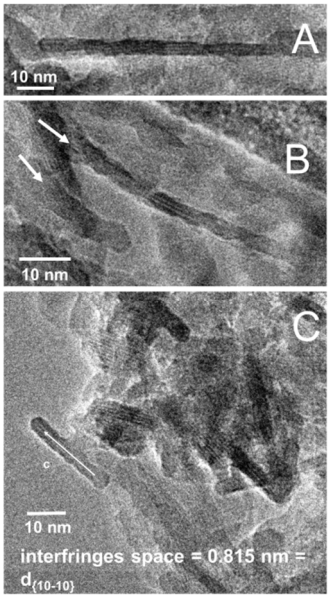

Fig. 3. HR-TEM images representative of the overall aspect of cit-Ap-4h. Original magnification: 150k×.

In agreement with XRPD and SAED, the particles maturated after 96 h (cit-Ap-96h) exhibited more clear fringes running along the *c*-axis, regularly spaced of ca. 0.815 nm, supporting the increase of crystallinity (Fig. 4). These particles appeared elongated along the *c*-axis, with sizes ranging from 20 to 50 nm (Figs. 4A,B) and in some cases up to 80-100 nm (Fig. 4C). Inspections at higher magnifications revealed that lattice fringes due to (10-10) planes ran uninterrupted parallel to the *c*-axis (Fig. S5, ESI†). Moreover, some facets of the *a*(*b*)-planes (*e. g.*, (0-110) facet in Fig. S5A, ESI†) exhibited stepped surfaces indicating that they grew (mediated by the ACP-to-crystalline transformation) following a classical layer-by-layer mechanism.

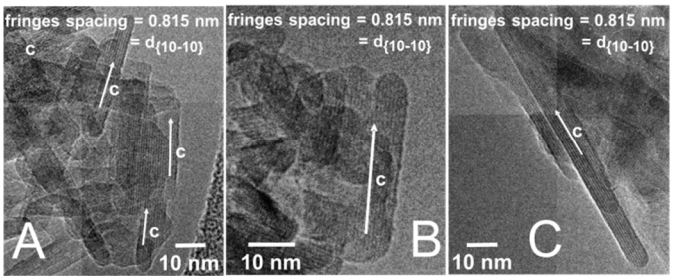

Fig. 4. HR-TEM images representative of the overall aspect of cit-Ap-96h. Original magnification: 150k×.

Figure 5 represents the histograms with the width and length of cit-Ap synthetized at different maturation times. Data were obtained by HR-TEM observations, analysing *ca.* 300 particles per sample. The length of particles with the highest frequency distribution slightly increased as a function of maturation time while the width remained nearly constant. Comparing the values of length and width evaluated by HR-TEM with those of the crystal domains measured by synchrotron XRTS (length: 16.6 ± 7.9 and 14.4 ± 9.6 nm, width 8.6 ± 1.3 and 10.3 ± 2.3 nm for 4h and 96 h, respectively; data extracted from reference 9), it was clearly observed that most of cit-Ap-4h and 96h particles were longer than the crystalline domains, while they had similar values of width. Moreover, after 96 h the shortest particles (0-20 nm) were still present, indicating that they did not dissolve during the maturation process. This fact and the discrepancy between data by HR-TEM and XRTS validated the formation of oriented aggregates along the *c*-axis composed of re-arranged crystalline domains. The thickness of the particles, measured by AFM (Fig. S6, ESI†), varied from 5.3 ± 1.1 to 13.5 ± 4.1 nm between 1 and 96 h of maturation, confirming the formation of platy-shaped nanoparticles.[9]

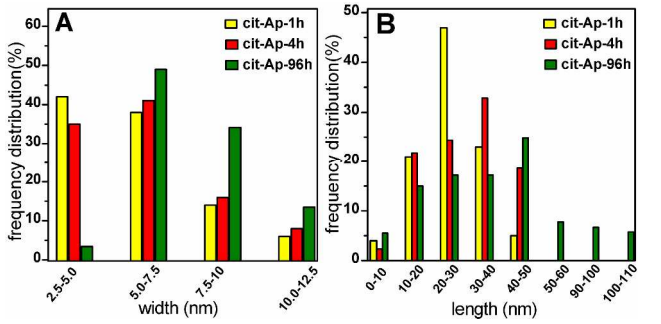

Fig. 5. Histograms of the distributions of (A) width and (B) length of cit-Ap-1h (yellow bars), cit-Ap-4h (red bars) and cit-Ap-96h (green bars).

According to our and previous results[9] crystallization of cit-Ap starts with the formation of platy ACP stabilized by adsorbed citrate (Fig. 6A). Increasing the maturation time ACP transforms into crystalline domains from the inner to the outer of the platy particles (Fig. 6B). Recent works showed that Ap crystallization from ACP may start at the inter-particles boundary, at the ACP-solution interface or inside the ACP, depending from the experimental conditions.[13] Once the Ap is formed, citrate is attached only to specific faces. It was recently demonstrated that citrate can strongly bind only the calcium of the faces of the *a(b)*-planes (faces parallel to the *c*-axis), stopping further growths in these directions and controlling thickness and width of the platy nanocrystals.[6a,9] This interaction occurs because the distance between two calcium ions in the hexagonal faces matches the distance between the carboxylate groups of citrate.[6a] At this point, the uniaxial alignment of crystalline subunits along the *c*-axis takes place (Fig. 6C). OA has been proposed to occur in three main stages: (i) aggregation, (ii) crystallographic alignment, and (iii) coalescence.[12,14] In our system Ap subunits can interact each other by Van der Walls or hydrogen bonding interactions[15] through the (0001) faces (head-tail attachment) since they are non-covered by citrate and thus the primary subunits can be in the crystallographic register with respect to the neighbouring crystals (Fig. 6D). The driving force of this process is the reduction of the overall crystal surface energy to lower the contribution of unsatisfied surface bond.[15] Citrate adsorbed on the faces of the *a(b)*-plane eliminates high-energy facets forcing the interaction between the (0001) faces. At the highest maturation time

CrystEngComm Accepted Manuscript

Fig. 6. Proposed model for the amorphous-to-crystalline transformation mechanism and for the OA of primary subunits to form elongated crystals.

solid-state re-arrangement of the subunits takes place through the growth of two (0001) adjacent faces, acting as glue, leading to the formation of elongated crystals (Fig. 6E), as previously proposed.[16] At this stage water and organic molecules entrapped between the primary particles can be removed allowing their fusion.[14] Indeed, the amount of structural water decreased between 4 and 96 h, whereas the amount of citrate remained constant (Table S2, ESI†). This finding confirms that the subunits faces involved in the fusion are citrate free.

In conclusion citrate plays a key dual role of: i) driving a growth pathway *via* an amorphous precursor stabilizing ACP at the early stage; ii) controlling nanocrystals size by adsorption on the *a(b)*-plane faces. HR-TEM observations combined with the analysis of crystalline domain sizes (measured by XRTS[9]) suggested a solid-state re-organization of the primary nanocrystals forming elongated multi-domain nanoparticles. This morphological and structural evolution cannot be related to an Ostwald ripening (OR) process involving a dissolution–recrystallization process since hydroxyapatite is insoluble in aqueous solution at pH higher than 6 even at 80 °C (Table S1, ESI†). Moreover, in agreement with our system where citrate is strongly attached to Ap, the stable adsorption of organic molecules induces the OA crystal growth mechanism at expenses of the OR process, because they slow down the particles dissolution in solution, so that the OR is thermodynamically prohibited.[12b] A similar solid-state OA growth mechanism has been already observed for TiO_2 and MnO_2.[3a,17] An analogous mechanism could also occur in bone mineralization where citrate, alone or in synergy with macromolecules, might play the key role of controlling size and morphology of Ap. This work opens also new perspectives in the use of organic molecules to mediate the Ap crystallization for a rational design of advanced biomaterials with controlled size and optimised performances.

This work was supported by the projects: SMILEY (NMP4-SL-2012-310637), MINECO co-funded with FEDER (MAT2011-28543 and Factoría de Cristalización) and the CEI-BioTic (mP_BS_8, UGR).

Notes and references

[a]*Istituto di Scienza e Tecnologia dei Materiali Ceramici (ISTEC), Consiglio Nazionale delle Ricerche (CNR), Via Granarolo 64, 48018 Faenza. Italy. (*)E-mail: michele.iafisco@istec.cnr.it;*

[b]*Laboratorio de Estudios Cristalográficos, Instituto Andaluz de Ciencias de la Tierra, IACT (CSIC-UGR), Av. Las Palmeras 4, 18100 Armilla, Spain. (*)E-mail: jmdl@lec.csic.es*

[c]*Dipartimento di Chimica & Centro Interdipartimentale "Nanostructured Interfaces and Surfaces"-NIS, Università degli Studi di Torino, Via P. Giuria 7, 10125 Torino, Italy.*

† Electronic Supplementary Information (ESI) available: Experimental details and XRPD, TEM, AFM, HR-TEM analyses, pH evolution and solution chemistry calculations. See DOI: 10.1039/c0000000/

(1) (a) S. Weiner, *J. Struct. Biol.* 2008, **163**, 229; (b) J. Gómez-Morales, M. Iafisco, J. M. Delgado-López, S. Sarda, and C. Drouet, *Prog. Cryst. Growth Ch.* 2013, **59**, 1.

(2) (a) S. Weiner and L. Addadi, *Annu. Rev. Mater. Res.* 2011, **41**, 21; (b) L. B. Gower, *Chem. Rev.* 2008, **108**, 4551.

(3) (a) R. L. Penn and J. F. Banfield, Science 1998, **281**, 969; (b) J. F. Banfield, S. A. Welch, H. Zhang, T. T. Ebert and R. L. Penn, *Science* 2000, **289**, 751.

(4) (a) J. D. Chen, Y. J. Wang, K. Wei, S. H. Zhang and X. T. Shi, *Biomaterials* 2007, **28**, 2275; (b) L. Hao, H. Yang, N. Zhao, C. Du and Y. Wang, *Powder Technol.* 2014, **253**, 172.

(5) (a) J. Tao, H. Pan, Y. Zeng, R. Xu and R. Tang, *J. Phys. Chem. B* 2007, **111**, 13410; (b) B. Palazzo, D. Walsh, M. Iafisco, E. Foresti, L. Bertinetti, G. Martra, C. L. Bianchi, G. Cappelletti and N. Roveri, *Acta Biomater.* 2009, 5, 1241; (c) L. Wang, X. Guan, H. Yin, J. Moradian-Oldak and G. H. Nancollas, *J. Phys. Chem. C* 2008, **112**, 5892.

(6) (a) Y. Y. Hu, A. Rawal and K. Schmidt-Rohr, *Proc. Natl. Acad. Sci.* 2010, **107**, 22369; (b) D. Reid, M. Duer, G. Jackson, R. Murray, A. Rodgers and C. Shanahan, *Calcif. Tissue Int.* 2013, 1; (c) J. M. Delgado-López, M. Iafisco, I. Rodríguez, A. Tampieri, M. Prat and J. Gómez-Morales, *Acta Biomater.* 2012, **8**, 3491.

(7) E. Davies, K. H. Müller, W. C. Wong, C. J. Pickard, D. G. Reid, J. N. Skepper and M. J. Duer, *Proc. Natl. Acad. Sci.* 2014, **111**, 1354.

(8) J. Gómez-Morales, J. M. Delgado-López, M. Iafisco, A. Hernández-Hernández and M. Prat, *Cryst. Growth Des.* 2011, **11**, 4802.

(9) J. M. Delgado-López, R. Frison, A. Cervellino, J. Gómez-Morales, A. Guagliardi and N. Masciocchi, *Adv. Funct. Mater.* 2014, **24**, 1090.

(10) Y. Chen, W. Gu, H. Pan, S. Jiang and R. Tang, *CrystEngComm* 2014, **16**, 1864.

(11) J. Mahamid, A. Sharir, L. Addadi and S. Weiner, *Proc. Natl. Acad. Sci.* 2008, **105**, 12748;

(12) (a) R. L. Penn and J. A. Soltis, *CrystEngComm* 2014, **16**, 1409. (b) J. Zhang, F. Huang and Z. Lin, *Nanoscale* 2010, **2**, 18.

(13) H. Pan, X. Y. Liu, R. Tang and H. Y. Xu, *Chem. Commun.* 2010, **46**, 7415.

(14) N. D. Burrows, C. R. H. Hale and R. L. Penn, *Cryst. Growth Des.* 2013, **13**, 3396.

(15) X. Xue, R. L. Penn, E. R. Leite, F. Huang and Z. Lin, *CrystEngComm* 2014, **16**, 1419.

(16) R. Rodriguez-Clemente, A. Lopez-Macipe, J. Gomez-Morales, J. Torrent-Burgues and V. M. Castano. J. Eur. Ceram. Soc. 1998, **18**, 1351.

(17) S. Patra, C. Davoisne, S. Bruyère, H. Bouyanfif, S. Cassaignon, P. L. Taberna and F. Sauvage, *Part. Part. Syst. Charact.* 2013, **30**, 1093.

CrystEngComm Accepted Manuscript

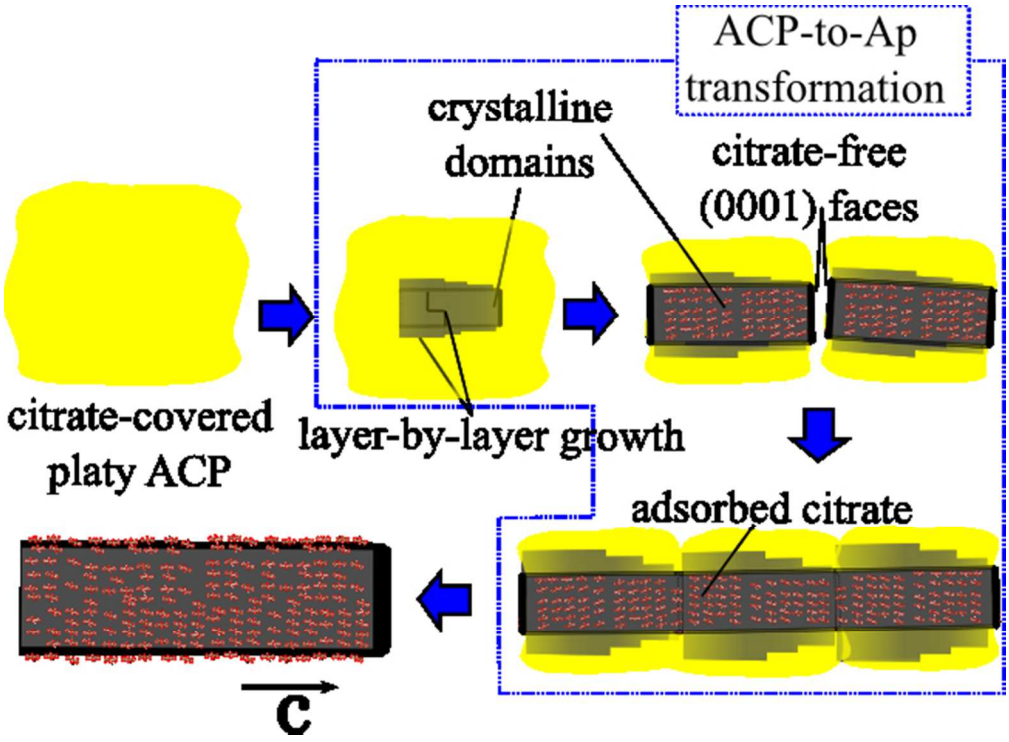

54x39mm (300 x 300 DPI)

CrystEngComm Accepted Manuscript

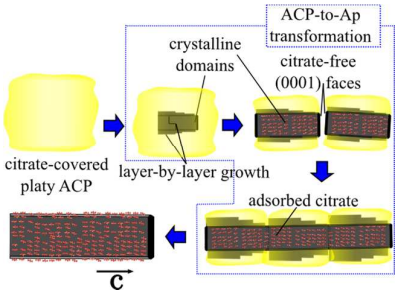

Citrate plays a dual role in the apatite crystallization: driving a growth pathway via an amorphous precursor and controlling the nanocrystals size by the non-classical oriented aggregation.

CrystEngComm Accepted Manuscript